Optics Communications 283 (2010) 2580–2587

Contents lists available at ScienceDirect

Optics Communications

journal homepage: www.elsevier.com/locate/optcom

Mueller matrix-based optimization of reflective type twisted nematic liquid crystal SLM at oblique incidences

R.S. Verma *, M.K. Swami, S.S. Manhas, P.K. Gupta

Laser Biomedical Applications and Instrumentation Division, Raja Ramanna Centre for Advanced Technology, Indore 452 013, India

ARTICLE INFO

Article history:
Received 18 August 2009
Received in revised form 14 February 2010
Accepted 14 February 2010

Keywords:
Spatial light modulators
Mueller matrix
Phase modulation
Holographic optical tweezers

ABSTRACT

Mueller matrix measurements were used to characterize the polarization properties of liquid crystal-based reflective type twisted nematic (TN) special light modulator (SLM) at oblique incidence of the laser beam. The experimentally obtained Mueller matrices were used to obtain the combination of polarization optics required to optimize it for phase only modulation. The results indicate that minimum intensity modulation is obtained with the use of a polarizer followed by a quarter wave plate (QWP) in polarization state generator (PSG) arm and a QWP followed by an analyzer in polarization state analyzer arm (PSA). Polarization parameters such as retardance, rotation and depolarization were calculated from the experimentally obtained Mueller matrices using polar decomposition method at different angle of incidences of the laser beam and the results has been discussed. The similarity between retardance and depolarization curve as a function of address voltage of TNSLM indicated that depolarization is mainly associated with errors in retardance values. Further, spectral Mueller matrix measurements were used to obtain intensity modulation response in the range of wavelengths 450–700 nm for broadband applications.

1. Introduction

Liquid crystal (LC) spatial light modulators are widely used in optical processing systems for dynamical control of amplitude and phase of light wave fronts. A large variety of applications such as diffractive optical element in holographic optical tweezers [1], optical storage [2], dynamic lenses [3] and adaptive optics [4] require it to work in phase modulation regime with a linear phase modulation of 2π with respect to the addressed gray level of SLM. This can be conveniently achieved with parallel aligned (PA) liquid crystal SLM where all the liquid crystal molecules are aligned parallel to each other. In this case application of electric field across the liquid cell results in a change of refractive index in response to the tilt of the LC molecules, which leads to phase modulation with no intensity modulation. On the other hand in twisted nematic (TN) type SLM's, the optic axis (director of the LC molecule) of LC cell layers is helically aligned across the LC cells. On application of voltage across the TNSLM, apart from the tilt of the molecules along the axis there is also a twist of molecules about the axis of SLM. This leads to coupled amplitude and phase modulations. Since TNSLM are cheaper and more readily available (mass production motivated by its display applications) there has been interest in characterization of the polarization parameters and finding appropriate configuration of the polarization state generator (PSG) and the polarization state analyzer (PSA) to achieve phase only modulation mode of the TNSLM. This can be done in two ways; one approach [5] is to measure amplitude and phase modulation response of the TNSLM for each configuration generated by the various combinations of the PSG and PSA. But this method is time consuming and will be more complex if to more effectively decouple intensity and phase modulation response, quarter wave-plates (QWP) are also included for generating elliptic polarization state [6]. The other approach [7–10] is to first model the optical behavior of the TNSLM and then use this model to find out the optimum orientation of the PSG and PSA for phase only response. For determining the polarization parameters of TNSLM, 2×2 Jones matrix has been used, however the applicability of Jones matrix formalism is questionable since in Twisted Nematic liquid crystal-based systems, the depolarization has been shown to be in the range of 2–9% [11]. Mueller matrix description is therefore more appropriate for the characterization of polarization parameters of TNSLMs and has indeed been used to characterize the transmitive type TNSLM's [6]. Since the reflective type SLM's are receiving more attention due to the fast response as compare to transmitive type, there have also been some attempts [12,13] to characterize reflective type TNSLMs at normal/quasi normal ($\sim$2–5°) incidences. However for many beam shaping applications including that for holographic optical tweezers (HOT), it would be useful if oblique incidence is used as it provides more space for the set up and also allows free access to place the polarization optics for different operating modes of the TNSLM. Further, the use of

* Corresponding author. Tel.: +91 731 2488443; fax: +91 731 2488425.
E-mail address: rsverma@rrcat.gov.in (R.S. Verma).

0030-4018/$ - see front matter © 2010 Elsevier B.V. All rights reserved.
doi:10.1016/j.optcom.2010.02.032

reflective type TNSLM's in oblique incidence geometry offers two other important advantages first, polarization sensitive cubic beam splitter is not required to separate the incident and reflected laser light that is required for normal incidence geometry and secondly the retardation optics can be placed independently in the input and output path for minimizing intensity modulation [14]. Recently some attempts [15–18] have also been made to characterize and optimize the TNSLM at large oblique incidences.

In this paper, we discuss the use of the Mueller matrix-based approach for characterization of polarization properties of reflective type TNSLM at oblique incidences of the beam and finding an optimum combination of polarization optics for achieving phase only modulation. Using the polar decomposition [19] of experimentally measured Mueller matrices for the characterization of polarization properties of reflective type TNSLM, we studied the dependence of the diattenuation, depolarization, linear retardance and rotation on the angle of incidence of the laser beam. The polar decomposition results enable us to conclude that the depolarization is mainly caused by the variation in linear birefringence. We have also studied, in detail, the wavelength response of the TNSLM for 45° angle of incidence in the wavelength range of 450–700 nm and discussion of results has been presented. The measured Mueller matrices were used to find out the best combination of polarization optics for minimizing the intensity modulation over a broad wavelength range.

2. Set up and method

2.1. Measurement of Mueller matrix

The schematic of the experimental set up used for the measurement of the Mueller matrix parameters of a Twisted Nematic SLM (LC-R 2500, Holoeye Photonics, Germany) is shown in Fig. 1a. The TNSLM is a 45° twisted nematic type spatial light modulator based on LCoS display, with XGA resolution (1024 × 768 pixels), having squire pixels of 19 μm pixel pitch and fill factor of 93%, with digitally controlled 256 (0–255) gray levels and phase modulation capability of $\sim 2\pi$ up to 700 nm. For measurements at single wavelength the output from a frequency doubled diode pumped Nd:YVO_4 laser (532 nm, cw Verdi, Coherent Inc., USA), was used to illuminate the TNSLM after passing through a fixed polarizer P1 and a rotatable QWP1 (532 nm) which act as a PSG. The polarization state analyzer, comprising of a rotating QWP2 (532 nm) followed by a fixed polarizer P2, was used to analyze the reflected light form the TNSLM. A power meter (Coherent Inc., USA) was used to measure the intensity of the laser light coming from PSA. For studying the behavior of the TNSLM at oblique incidences the TNSLM, PSA and power meter were mounted on a rotational stage. For spectral Mueller matrix measurement, collimated white light output from a 1 kW Xe lamp (Sciencetech, 201–1K, Canada) was used to illuminate the TNSLM. For these measurements the QWPs designed for 632 nm were used in both PSG and PSA. A fiber optic probe whose distal end was coupled to a spectrometer (Avaspec-2048TEC-FT, Avantes, Netherland) was used to record the reflected intensity.

Measurement of Mueller matrix using PSG/PSA approach requires a set of four incident polarization states (generated using four orientations of QWP1 with respect to P1) in the input and detection of intensities at four different polarization states (using four orientations of QWP2 with respect to P1) at the output. The PSG and PSA can therefore be written as:

$$\mathrm{PSG} = \begin{pmatrix} 1 & 1 & 1 & 1 \\ C^2_{\theta_{in}1} + S^2_{\theta_{in}1} C_\delta & C^2_{\theta_{in}2} + S^2_{\theta_{in}2} C_\delta & C^2_{\theta_{in}3} + S^2_{\theta_{in}3} C_\delta & C^2_{\theta_{in}4} + S^2_{\theta_{in}4} C_\delta \\ S_{\theta_{in}1} C_{\theta_{in}1} (1 - C_\delta) & S_{\theta_{in}2} C_{\theta_{in}2} (1 - C_\delta) & S_{\theta_{in}3} C_{\theta_{in}3} (1 - C_\delta) & S_{\theta_{in}4} C_{\theta_{in}4} (1 - C_\delta) \\ S_{\theta_{in}1} S_\delta & S_{\theta_{in}2} S_\delta & S_{\theta_{in}3} S_\delta & S_{\theta_{in}4} S_\delta \end{pmatrix} \quad \text{(i)}$$

$$\mathrm{PSA} = \begin{pmatrix} 1 & -(C^2_{\theta_o 1} + S^2_{\theta_o 1} C_\delta) & -C_{\theta_o 1} S_{\theta_o 1} (1 - C_\delta) & S_{\theta_o 1} S_\delta \\ 1 & -(C^2_{\theta_o 2} + S^2_{\theta_o 2} C_\delta) & -C_{\theta_o 2} S_{\theta_o 2} (1 - C_\delta) & S_{\theta_o 2} S_\delta \\ 1 & -(C^2_{\theta_o 3} + S^2_{\theta_o 3} C_\delta) & -C_{\theta_o 3} S_{\theta_o 3} (1 - C_\delta) & S_{\theta_o 3} S_\delta \\ 1 & -(C^2_{\theta_o 4} + S^2_{\theta_o 4} C_\delta) & -C_{\theta_o 4} S_{\theta_o 4} (1 - C_\delta) & S_{\theta_o 4} S_\delta \end{pmatrix} \quad \text{(ii)}$$

where subscript '$\theta_{in}i$' and '$\theta_o i$' (i = 1, 2, 3, 4) corresponds to the orientation angles of fast axis of QWP1 and QWP2, respectively, and $C_\theta = \cos 2\theta$, $S_\theta = \sin 2\theta$, $C_\delta = \cos \delta$, $S_\delta = \sin \delta$, with δ being the linear retardance of the QWPs. For spectral Mueller matrix measurements, PSG and PSA were adjusted to account the wavelength

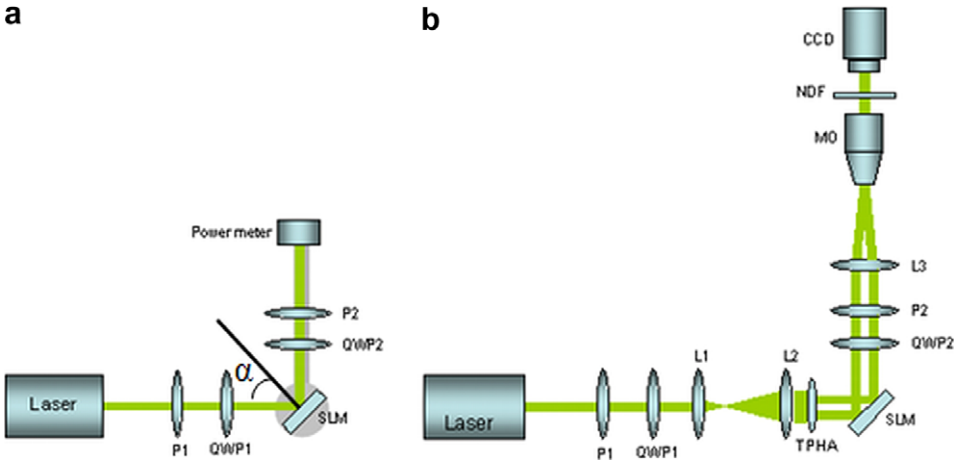

Fig. 1. Schematics of the setup for (a) Mueller matrix measurement at varying angle of incidence of the input beam and (b) phase modulation measurement of the reflective type TNSLM for 45° angle of incidence for the laser beam.

dependent retardance (δ) of wave plate at each wavelength (450–700 nm) [20].

In the whole study the angles were measured with respect to the laboratory vertical looking towards the propagation direction of the beam. The polarizer (P1) was kept vertical and polarizer–analyzer (P1 and P2) were kept crossed with respect to each other. The 16 measured intensities matrix (M_i) is related to the sample Mueller matrix (M_s) as [21]

$$M_i = \mathrm{PSA} \cdot M_s \cdot \mathrm{PSG} \tag{iii}$$

The Mueller matrix of the sample (M_s) can also be written in 16×1 form

$$M_{ivec} = W \cdot M_{svec} \tag{iv}$$

where W is 16×16 matrix given by Kronecker product [22] of PSA with transpose of PSG

$$W = \mathrm{PSA} \otimes \mathrm{PSG}^T \tag{v}$$

We term the matrix W as the measurements matrix since its operation on a 16×1 column vector M_{svec} gives a 16×1 column vector (M_{ivec}) with measured intensity as its elements. The measurement matrix W is completely determined by the retardance and the orientation of the fast axis of the QWPs used.

So the Mueller matrix (M_{svec}) of the sample is determined by

$$M_{svec} = W^{-1} M_{ivec} \tag{vi}$$

For inverse computation (in Eq. (vi)), the determinant of the W must be non-zero. Therefore the orientation angles of QWPs were optimized such that the determinant of the measurement matrix is maximum. The determinant of the measurement matrix was computed for all possible set of four equally spaced orientations of QWP in PSG and PSA. The QWP orientation angles at which the determinant of 'W' was maximum, were taken for Muller matrix measurements of the TNSLM. In this case the optimum values for the orientation angles of QWPs with respect to transmission axis of first polarizer P1 were 35°, 70°, 105° and 140°.

The Mueller matrix measurements were done at 16-evenly spaced address voltages (0, 16, 33, ...) spanning the entire range of TNSLM gray level. For the spectral measurements Mueller matrix at each wavelength was calculated by adjusting the PSG and PSA to account for the wavelength dependent retardance of wave plate at each wavelength in the range 450–700 nm.

2.2. Minimum intensity modulation computation

The intensity modulation response of TNSLM with different possible configurations utilizing polarizer and wave plate on both sides of the TNSLM were estimated by using Mueller matrix measured at 16-evenly spaced address voltages. The output polarization state of the system after the PSA can be written as

$$S_O = M_{PO} M_{QO} M_J M_{QI} M_{PI} S_I \tag{vii}$$

where S_I and S_O are the input and output state stokes vector. M_{PO}, M_{QO}, M_J, M_{QI} and M_{PI} are the Mueller matrix of output polarizer, output QWP, TNSLM, input QWP and input polarizer, respectively. The input state polarization was taken as un-polarized, i.e.

$$S_I = [1 \quad 0 \quad 0 \quad 0] \tag{viii}$$

The intensity modulation for a given configurations was characterized by calculating variance of the first element of S_O as a function of grayscale value with different combination of input and output polarization states spanning whole range of orientations of polarizer/analyzer and QWPs

$$\sigma = \sqrt{\sum_{i=1}^{16} (\langle S_O\ (1)\rangle - S_{Oi}\ (1))^2 / 16} \tag{ix}$$

In all, for studying the intensity modulation of TNSLM at oblique incidence, three orientations 15°, 30° and 45° were studied. The orientation angles (denoted by 'α' in Fig. 1a) are the angle of incidences of the beam with respect to the normal at the surface of TNSLM. In each orientation of the TNSLM four configurations comprising different possible combination of polarizer, analyzer and QWP's were studied; (a) polarizer-TNSLM-analyzer (b) polarizer-QWP-TNSLM-analyzer (c) polarizer-TNSLM-QWP-analyzer and (d) polarizer-QWP-TNSLM-QWP-analyzer.

2.3. Single wavelength phase modulation measurement

The phase modulation was measured for the configuration with minimum intensity modulation using two-beam interferometry method. The schematic of the set up is shown in Fig. 1b. The beam was expanded using suitable lens combination and thereafter split in two parts by a two pinhole aperture (TPHA). For the phase shift measurement Phase cam software from Holoeye Photonics, Germany was used. With the help of this software the entire TNSLM region was vertically divided in two parts; the address voltage of half plane, considered as reference plane, is fixed and the address voltage of the other half plane is varied by varying the gray level from 0 to 255 by the software. Both parts of the incident beam coming from TPHA were made to incident on TNSLM in such a way that one part of the beam falls on reference plane and the other part on rest half of the plane. Both part of the beam after getting reflected from the TNSLM passed through the PSA and was focused by lens (L3). A 10 microscope objective was used to magnify the interference image. The images were recorded using a CCD connected with a computer.

3. Polar decomposition of Mueller matrix

Polar decomposition of Mueller matrix is a robust and efficient approach for the quantification of the polarization parameters of the optical media from measured Mueller matrix. The process for polar decomposition of experimentally measured Mueller matrix into Mueller matrices of a diattenuator M_D (component that causes different amplitude changes for its orthogonal eigen states), a retarder M_R (component that causes dephasing of two eigen states) and a depolarizer M_Δ (component that causes depolarization) has been described in details by Lu and Chipman [19] and others [21,23].

4. Results and discussion

4.1. Intensity modulation at oblique incidences of the beam for single wavelength

For all possible combinations of QWPs and polarizer orientation angles (denoted as 'βi' and 'βo' for polarizer and analyzer; γi and γo for input side QWP1 and output side QWP2, respectively) in all configurations the intensity modulation minima was calculated at 15°, 30° and 45° angle of incidence (α) of laser beam using Eq. (ix) and result is tabulated in Table 1. Among all the configurations (a–d) studied, the intensity modulation minima for 45° orientation of TNSLM was obtained when a polarizer followed by a QWP was placed at the input and a QWP followed by an analyzer was placed at the output of the TNSLM. Fig. 2 shows intensity modulation when TNSLM was oriented in 45° with respect to the incident beam and in the configuration QWP's were used on both the sides of TNSLM. In this configuration a total of four intensity modulation

Table 1
Minimum intensity modulation of TNSLM for different angle of incidence (α) of the input laser beam in different configurations (a–d).

Orientation (°) of TNSLM (α)	Configuration	QWP before TNSLM (°) (γi)	QWP after TNSLM (°) (γo)	Polarizer (°) (βi)	Analyzer (°) (βo)	Minimum intensity modulation (%)
15	Only polarizers			124	88	15
30	-do-			43	104	7
45	-do-			141	110	2
15	QWP before TNSLM	36		56	94	5
30	-do-	47		154	100	4
45	-do-	58		160	107	1.5
15	QWP after TNSLM		18	7	74	4
30	-do-		48	17	14	1.5
45	-do-		78	21	108	2
15	QWP on both side of TNSLM	10	23	103	84	2.5
30	-do-	16	46	107	10	1.5
45	-do-	22	52	18	2	0.5

minima were observed when the QWP's orientations were $\gamma i = 22°$ and $\gamma o = 52°$ and the polarizer, analyzer angles were $\beta i = 18°$ and $\beta o = 2°$.

The Poincare sphere depiction of intensity modulation by TNSLM allows visualization of the role of QWP's and polarizers in achieving optimum configuration for phase only modulation mode. The intensity transmitted for a state of polarization defined as

$$S_t = M_{QO} M_J M_{QI} M_{PI} S_I \quad (x)$$

through a polarizer at the output (M_{PO}) is given by a point on the equator is $\cos^2(L/2)$. L is the shortest length of the curve joining the two points (S_t and the second point representing the output polarizer orientation on the Poincare sphere) along the surface of Poincare sphere. Keeping the polarizer, QWP1 and QWP2 at the optimized orientation, output polarization states were generated for the 16-evenly spaced gray levels spanning the whole range of TNSLM. In Fig. 3, the output states are shown (circles) for optimized orientation and for some randomly chosen orientation of P_1, QWP1 and QWP2. In case the polarizers QWP1 and QWP2 are not in the optimized orientation, the distance of the output state (S_t) from the analyzer state is varying which means that the intensity of the light coming out of the analyzer will not be same as the component of polarization states along the analyzer axis will not be the same. Where as in the optimized case all the 16 states have nearly equal distances from the analyzer, i.e., the component of polarization states along the analyzer axis has small variation. So effectively by using polarizer, QWP1 and QWP2 we are trying to generate the output polarization states which will be symmetric to some point on the meridian of the Poincare sphere and the analyzer orientation will be that point on the meridian.

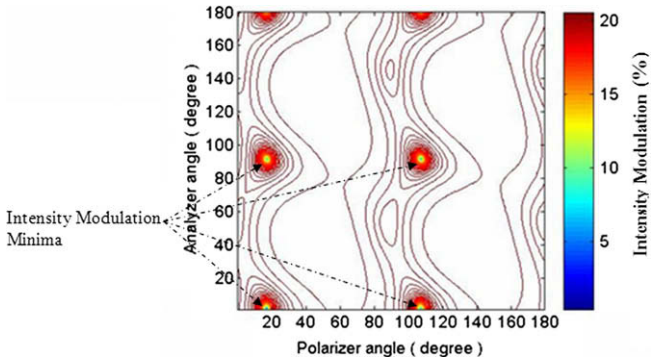

Fig. 2. Contour plot of intensity modulation from the TNSLM at different polarizer, analyzer angles when QWP1 was at 22° and QWP2 was at 52°.

Since the intensity modulation minima occurred when we used one QWP between polarizer and TNSLM and the other one between TNSLM and analyzer for 45° angle of incidence (α) of the laser beam, further studies were concentrated only for this orientation of the TNSLM.

4.2. Phase modulation measurement

Phase modulation measurement was pursued only at the four intensity modulation minima observed in configuration (d) at 45° orientation (α) of the TNSLM and is shown in Table 2. Among the four optimized polarization state of the PSG and PSA, two cases when the polarizer angle (βi) was at 18° and analyzer angle (βo)

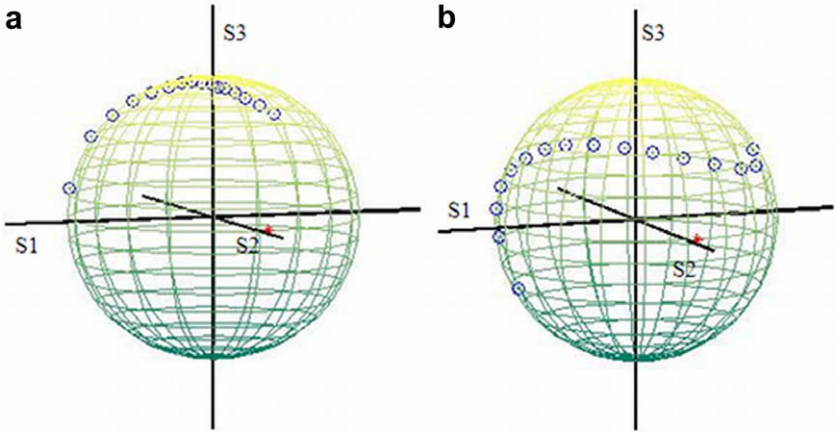

Fig. 3. Poincare sphere presentation of the intensity modulation in (a) optimized orientation (b) a random orientation of the polarizer, analyzer and quarter wave plate.

was at 2° and 92°, the linear phase modulation was ~2π with ±1% intensity modulation. Recently Lizana et al. [17] have also reported a similar approach to optimize the same TNSLM for phase only mode. However, for 45° orientation of the TNSLM under optimized condition of PSG and PSA, they could achieve ~240° phase modulation with much larger intensity modulation (~20%).

4.3. Diattenuation, linear retardance, circular retardance and depolarization dependence on angle of incidence

Following the polar decomposition approach developed by Lu and Chipman [19], we computed the polarization parameters; diattenuation, depolarization, and retardance from experimentally obtained Mueller matrix for TNSLM. The results are shown in Fig. 4 for different angle of incidences ($\alpha = 15°$, 30°, and 45°) of laser beam for 16 equally spaced gray levels from 0 to 255. As can be seen, for the whole range of gray scale of TNSLM, diattenuation and depolarization values are small (the maximum value of diattenuation is ~0.1 for $\alpha = 15°$ and the maximum depolarization is ~7% in gray level range around gray level 200 for $\alpha = 45°$) and the dominant contribution to the Muller matrix of TNSLM is from retardance. The observed variation of depolarization with angle of incidence (α) of laser beam is qualitatively similar to that obtained by Lizana et al. [17] and can be attributed to the scattering from the cell edges which is expected to increase with increasing angle of incidence. Further, the retardance range is large for small angle of incidence and decreases with increases in the angle of incidence which is also in qualitative agreement with previous report [17].

Following the approach described by Manhas et al. [21], we further decompose the retardance matrix to linear retarder matrix and circular retarder (rotator) matrix. The results are shown in Fig. 5 for different angle of incidences ($\alpha = 15°$, 30°, and 45°) as a function of gray levels. The linear retardance is seen to be large for small angle of incidence and decreases with increases in angle of incidence (α). The maximum linear retardance is ~175° at ~185 gray level for $\alpha = 15°$ and for $\alpha = 45°$ it is ~150° at ~120 gray level of TNSLM. The maximum value of circular retardance (rotation) caused by the TNSLM shifts towards higher gray level as the angle of incidence (α) increases. It is pertinent to emphasize here that since the diattenuation and depolarization values are small (maximum 0.1% and 7%, respectively), the TNSLM can be treated as a system consisting of the linear retarder followed by rotator at oblique incidence of the laser beam in agreement with previously reported result [24].

Table 2
Phase modulation response of TNSLM at various polarizer and analyzer orientation. For these measurements the QPW's are at 22° (γi) at 52° (γo), respectively.

Polarizer angle (βi)	Analyzer angle (βo)	Phase modulation
18	2	2.1 π
18	92	2.0 π
108	2	1.0 π
108	92	0.1 π

4.4. Depolarization behavior of TNSLM

In the liquid crystal-based devices depolarization is assumed to be mainly arising from the scattering due to the orientation fluctuation of the molecules. The other causes are the spatial averaging of the retardance within each pixel, electric field variations, edge effects in pixels and disclination in the liquid crystal [25]. The polar decomposition of the experimentally measured Mueller matrix shows that the depolarization of TNSLM follows the variation in

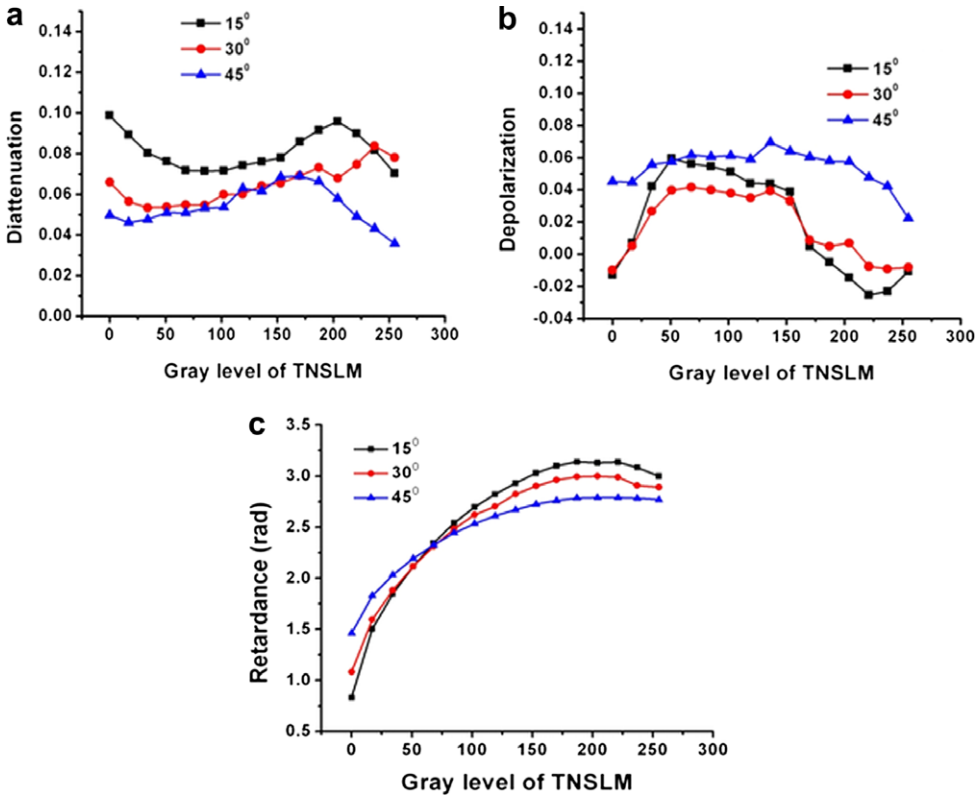

Fig. 4. Polar decomposition results of the Muller matrix of TNSLM measured at different angle of incidences (α) of the laser beam (a) diattenuation, (b) depolarization, and (c) retardance.

linear retardance as shown in Fig. 6. This suggests that among the different depolarizing factors variation in linear birefringence is the dominant factor for the depolarization effect caused by the TNSLM. Since the birefringence fluctuation is expected to grow in amplitude as birefringence increases, the depolarization is expected to follow the birefringence curve. Other studies [12] have also pointed out towards fluctuation of polarization state in time for light scattered from the TNSLM resulting from electric field fluctuations, which results in birefringence fluctuations.

4.5. Wavelength response of the TNSLM

TNSLM is widely used in adaptive optics systems, which require it to be characterized for the large wavelength range [26]. Wavelength dependence of TNSLM makes it difficult to use the same combination of polarization optics optimized for any particular wavelength to use for other wavelengths in the spectral range for which the TNSLM can give $\sim 2\pi$ phase modulation. We, therefore, studied the intensity modulation characteristics of TNSLM between the spectral range 450 and 700 nm to find out the wavelength regions where the TNSLM can be efficiently used in phase only modulation mode for 45° angle of incidence (α) of the laser beam. For this we used the spectral Mueller matrix measurement method to calculate the Mueller matrix for wavelengths in the wavelength range 450–700 nm at a step size of ~5 nm. For each wavelength studied, the optimized orientations of the polarizers and QWP's for minimum intensity modulation were calculated and are shown in Fig. 7. When only polarizers were used, the intensity modulation was 4–16% whereas in case a QWP was used at one side of the TNSLM, the intensity modulation was better (~4%) and more uniform.

Further, some applications of TNSLM with pulse laser systems require it to behave uniformly for the spectral bandwidth of the pulsed lasers systems. So the broad band wavelength response of the TNSLM was studied from 450 to 700 nm at step size of ~5 nm. To achieve the minimized broadband intensity modulation, the suitable configuration of polarization optics were calculated for each wavelength and thereafter for each optimized orientation the intensity modulation was calculated for the whole wavelength range (450–700 nm). Fig. 8 shows the broad band response of the TNSLM for different configurations (a–c) for 45° angle of incidence of the laser beam. In case we used only polarizers, the intensity modulation minima (~5%) corresponded to ~20 nm bandwidth as shown in Fig. 8a. Fig. 8b and c shows that the intensity modulation response of the TNSLM is improved when we used QWP on either side of the TNSLM. In case QWP was used before the TNSLM, the intensity modulation minima corresponded to ~20 nm bandwidth where as in case QWP was used after the TNSLM the intensity modulation minima corresponded to ~10 nm bandwidth with

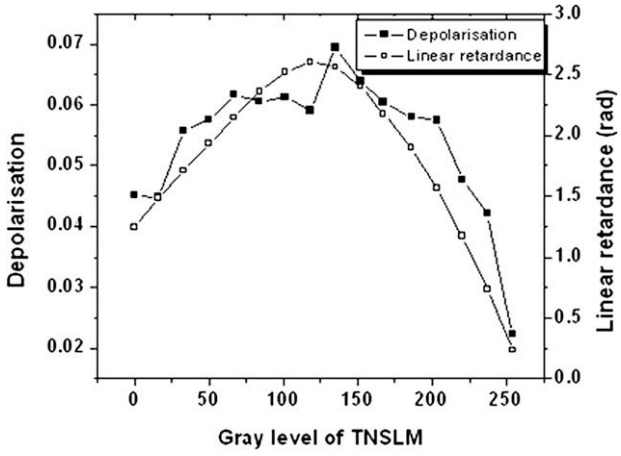

Fig. 6. Depolarization and the linear retardance of TNSLM for 45° angle of incidence.

intensity modulation of ~2% in both the cases. To have uniform intensity modulation of the TNSLM for a given wavelength range, we need to excite it with a polarization close to eigen polarization state of TNSLM. It is known that the eigen polarization state of the TNSLM are elliptic [27], so the elliptic polarization state will be more suitable as compared to the linearly polarized light. When QWP is used before the TNSLM, the input for the TNSLM is elliptically polarized light where as in case we used QWP after the TNSLM; the input for the TNSLM is linearly polarized light. We also studied the configuration having two QWP one on each side of the TNSLM. Though in this configuration the intensity modulation minima were lower than other configurations, the minima had lesser wavelength spread. So this configuration is not suitable for broadband application of the TNSLM with laser systems having spectral bandwidth of a few nm.

5. Conclusion

We have shown the use of Mueller matrix description of TNSLM for the optimization and polarization characterization of TNSLM. The 16 experimentally measured Mueller matrices corresponding to different address voltages of the TNSLM were used to estimate the minimum intensity modulation configuration employing quarter wave-plates and polarizers. The 45° orientation (α) of TNSLM corresponds to intensity modulation minima among the other oblique incidences in configuration having polarizer and QWP on both sides. Our studies on the depolarization response of the TNSLM (using polar decomposition of Mueller matrices) suggest that the pixel to pixel linear retardance fluctuations to be the major

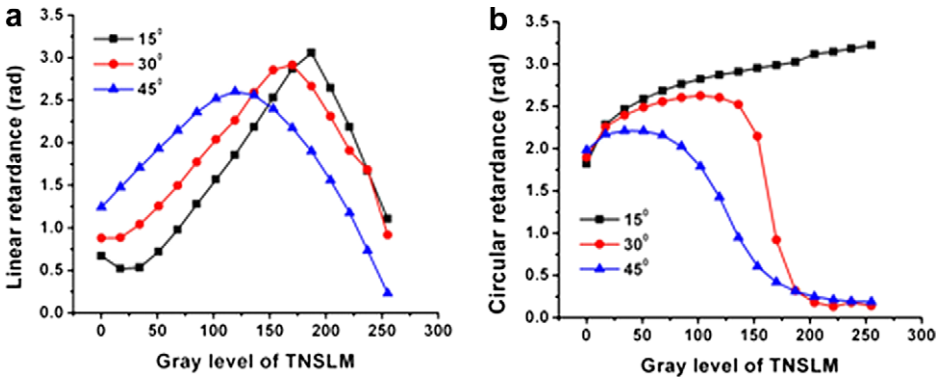

Fig. 5. Linear retardance (a) and circular retardance (b) variation with gray level of TNSLM for different angle of incidences (α) of laser beam.

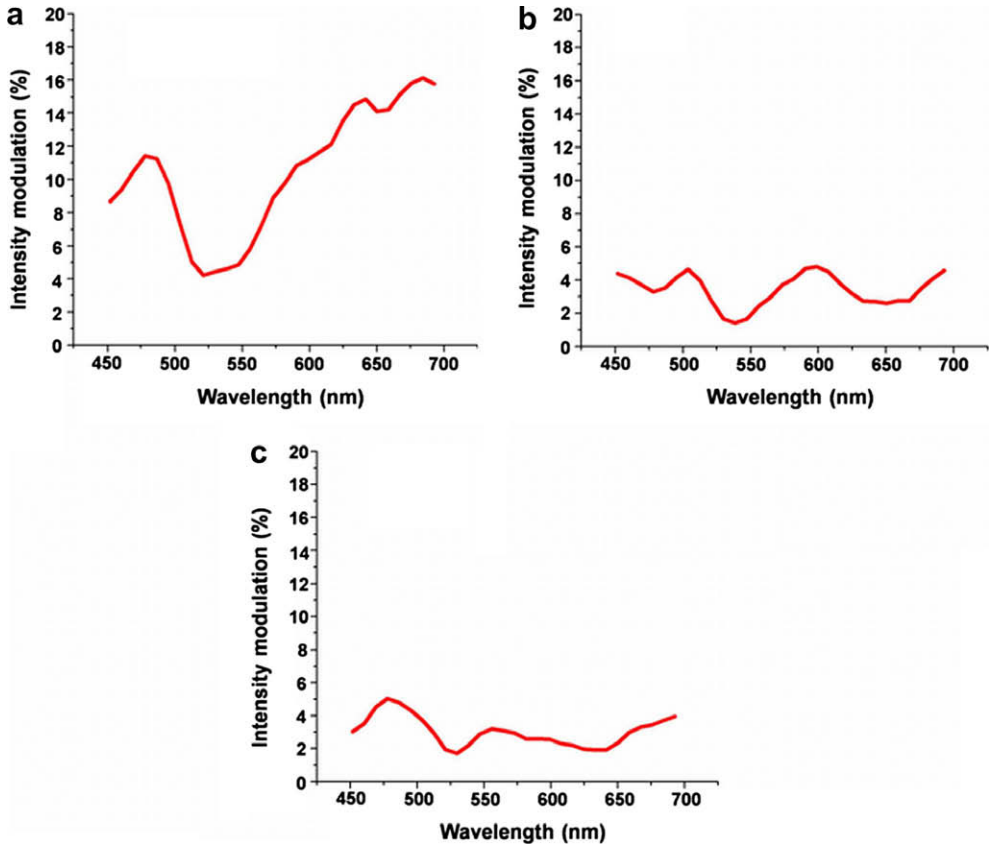

Fig. 7. Intensity modulation of TNSLM in different configurations (a) only polarizers (b) QWP before TNSLM (c) QWP after TNSLM; for multiple wavelengths.

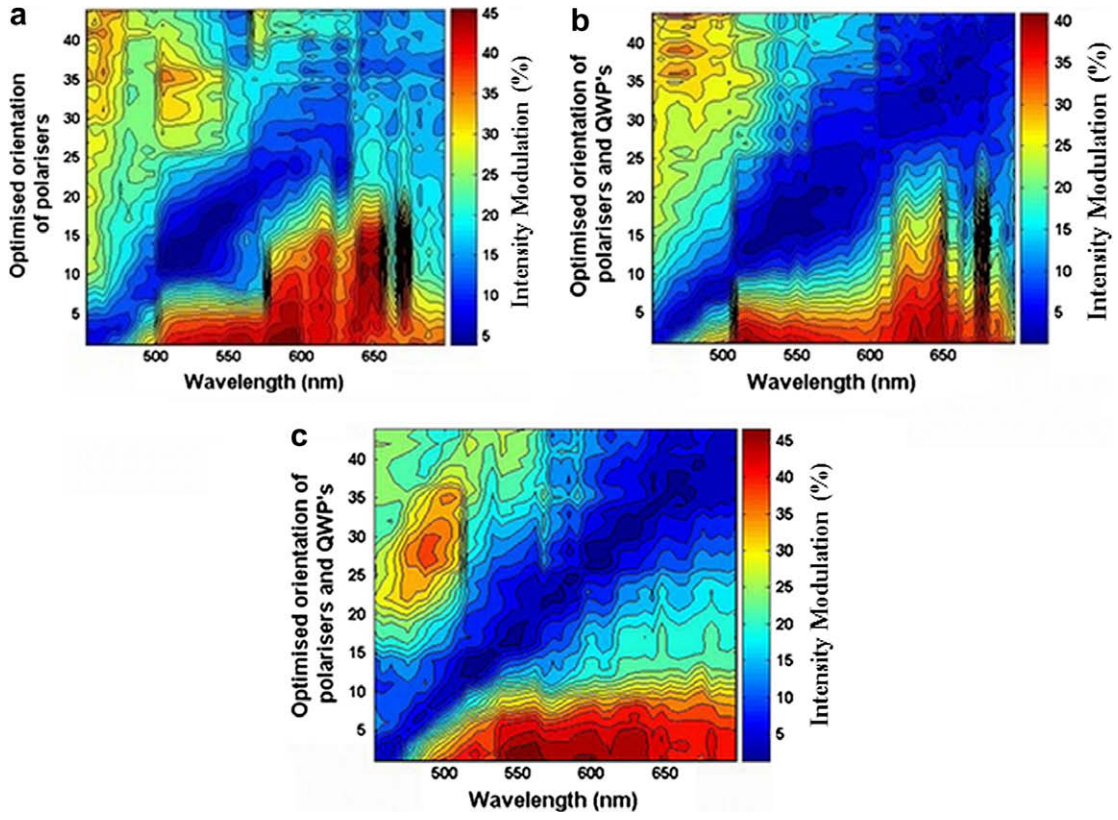

Fig. 8. The wavelength response of the TNSLM for the case (a) when only polarizers were used on both side of TNSLM (b) when QWP was used before the TNSLM along with the polarizers and (c) when QWP was used after the TNSLM along with the polarizers. Here 'optimized orientations of polarizers and QWP' represented by numbers. Each number is representative of one optimized combination of polarizes and QWP's for minimum intensity modulation for one wavelength.

contributor to the depolarization. Multi wavelength measurements were performed to see the suitability of the combination of polarization optics for minimum intensity modulation. We showed that the configuration with QWP at either side is better among different configurations for the broadband applications. This method can be used at any oblique incidence of the laser beam with respect to the TNSLM front surface.

Acknowledgement

Authors would like to thank H.S. Patel for useful discussion and a careful reading of the manuscript.

References

[1] Eric R. Dufresne, Gabriel C. Spalding, Matthew T. Dearing, Steven A. Sheets, David G. Grier, Rev. Sci. Instrum. 72 (2001) 1810.
[2] H.J. Coufal, D. Psaltis, B.T. Sincerbox (Eds.), Holographic Data Storage, Springer-Verlag, Berlin, 2000.
[3] V. Laude, Opt. Commun. 153 (1998) 134.
[4] Chao Li, Mingliang Xia, Quanquan Mu, Baoguang Jiang, Li Xuan, Zhaoliang Cao, Opt. Express 17 (2009) 10774.
[5] E. Martín-Badosa, A. Carnicer, I. Juvells, S. Vallmitjana, Meas. Sci. Technol. 8 (1997) 764.
[6] J.L. Pezzanitti, R.A. Chipman, Opt. Lett. 18 (1993) 1567.
[7] K. Lu, B.E.A. Saleh, Opt. Eng. 29 (1990) 240.
[8] Makoto Yamauchi, Appl. Opt. 44 (2005) 4484.
[9] Makoto Yamauchi, Tomoaki Eiju, Opt. Commun. 115 (1995) 19.
[10] I. Moreno, P. Velasquez, C.R. Fernandez-Pousa, M.M. Sanchez-Lopez, F. Mateos, J. Appl. Phys. 94 (2003) 3697.
[11] J. Larry Pezzaniti, Stephen C. McClain, Russell A. Chipman, Shih-Yau Lu, Opt. Lett. 18 (1993) 2071.
[12] A. Márquez, I. Moreno, C. Iemmi, A. Lizana, J. Campos, M.J. Yzuel, Opt. Express 16 (2008) 1669.
[13] P. Clemente, V. Durán, L. Martínez-León, V. Climent, E. Tajahuerce, J. Lancis, Opt. Express 16 (2008) 1965.
[14] E. Marťın-Badosa, M. Montes-Usategui, A. Carnicer, J. Andilla, E. Pleguezuelos, I. Juvells, J. Opt. A: Pure Appl. Opt. 9 (2007) S267.
[15] R.S. Verma, M.K. Swami, S. Manhas, P.K. Gupta, National Laser Symposium-2007, Held at M.S. University of Baroda, Vadodara, Gujarat on 16–20 December, 2007.
[16] R.S. Verma, M.K. Swami, S. Manhas, P.K. Gupta, Optics with in Life Sciences-10 Held at Singapore, 2–4 July, 2008, p. 28.
[17] A. Lizana, N. Martín, M. Estapé, E. Fernández, I. Moreno, A. Márquez, C. Iemmi, J. Campos, M.J. Yzuel, Opt. Express 17 (2009) 8491.
[18] A. Lizana, A. Márquez, I. Moreno, C. Iemmi, J. Campos, M.J. Yzuel, J. Eur. Opt. Soc., Rapid Pub. 3 (2008). 08011 1-6.
[19] S.-Y. Lu, R.A. Chipman, J. Opt. Soc. Am. A 13 (1996) 1106.
[20] M.K. Swami, S. Manhas, R.S. Verma, H.S. Patel, P.K. Gupta, A Simple Approach for Spectral Mueller Matrix Polarimetry, unpublished manuscript.
[21] S. Manhas, M.K. Swami, P. Buddhiwant, N. Ghosh, P.K. Gupta, K. Singh, Opt. Express 14 (2006) 190.
[22] P. Yeh, C. Gu, Optics of Liquid Crystal Displays, John Wiley and Sons, 1999.
[23] F. Le Roy-Brehonnet, B. Le Jeune, Prog. Quan. Electron. 21 (1997) 109.
[24] S. Stallinga, J. Appl. Phys. 85 (1999) 3023.
[25] Justin E. Wolfe, Russell A. Chipman, Appl. Opt. 45 (2006) 1688.
[26] Gordon D. Love, Appl. Opt. 36 (1997) 1517.
[27] J.A. Davis, I. Moreno, T. Tsai, Appl. Opt. 37 (1998) 937.